Transport properties of multigrained nanocomposites with imperfect interfaces

Pier Luca Palla, Stefano Giordano

Pier Luca Palla and Stefano Giordano

View Online   Export Citation   CrossMark

AIP Publishing

Transport properties of multigrained nanocomposites with imperfect interfaces

Pier Luca Palla and Stefano Giordano[a)]
Univ. Lille, CNRS, Centrale Lille, ISEN, Univ. Valenciennes, UMR 8520-IEMN, F-59000 Lille, France

Multigrained or polycrystalline composite materials have attracted a considerable attention due to their potential applications as advanced materials with outstanding thermal, mechanical, and electromagnetic properties. When the grains' morphology is displayed at the nanoscopic scale, the presence of imperfect interfaces plays a central role in determining the effective transport properties. Therefore, we develop here a self-consistent effective medium theory able to evaluate the influence of real contacts between the different phases of multigrained composite materials. This approach takes into account the classical interface schemes that have been introduced in literature, namely, the low and the high conducting interface models. The theoretical results have been compared with numerical and experimental data concerning the thermal conductivity of $(1-x)\text{Si} : x\text{Ge}$ mixtures and the electrical conductivity of $(1-x)\text{Li}_2\text{O} : x\text{B}_2\text{O}_3$ composites. *Published by AIP Publishing.*
[http://dx.doi.org/10.1063/1.4967316]

I. INTRODUCTION

The determination of the effective thermal, mechanical, and electromagnetic properties describing the physical behavior of heterogeneous materials is a crucial problem in modern material science.[1–4] In particular, the behavior of nanocomposites, multiphase solid materials where the microstructure is displayed at the nanoscopic scale, is remarkably important because of the recent multiple nanotechnological applications. In this case, several unusual physical properties can be attributed to the intensified fraction of interfaces or grain boundaries within these materials. As a matter of fact, the features of these interphase regions drive the size effects, i.e., the effects of the granulometry on the overall physical properties. Typically, in the classical macroscopic modeling, the interfaces are assumed to be perfect. For instance, in the context of the electrical conduction problem, it means that the electrical potential ϕ and the normal component of the current density $\vec{J}$ are continuous across any interface:[5,6] $[\![\phi]\!] = 0$ and $[\![\vec{J} \cdot \vec{n}]\!] = 0$, where the symbol $[\![f]\!]$ represents the jump of the function f across the interface. Of course, this is only an approximation that is valid in the case of small surface/volume ratio. In most of the cases with nanoscale microstructures, this approximation is no longer valid, and, therefore, it is important to take into consideration the specific properties of interfaces among the constituents. To this aim, two well-known zero-thickness interface models have been developed to describe two real limiting cases.

The first model is called *low conducting interface*, and it is based on the Kapitza resistance, introduced in the context of the thermal conduction.[7] According to this approach, $[\![\vec{J} \cdot \vec{n}]\!] = 0$, while the potential suffers a jump proportional to the local flux, $[\![\phi]\!] = -r\vec{J} \cdot \vec{n}$, where r is the Kapitza-like resistance. The second model, called *high conducting interface*, concerns the case of an interphase of very high

conductivity described by $[\![\phi]\!] = 0$, and by the normal component of the current density proportional to the surface Laplacian of the potential, $[\![\vec{J} \cdot \vec{n}]\!] = g\nabla_s^2\phi$, where g represents the interphase conductance. Several investigations on heterogeneous particulate materials with low[8–18] or high[11,17,19–23] conducting interfaces can be found in literature. Moreover, other models are based on an explicit interphase of finite thickness, and, therefore, they separately consider the inclusions, the interphase medium, and the matrix.[24–26] Recent results concern the integration of the low and high interface paradigms in more general models based on the T and Π lattice structures,[27,28] theories for composites with curvilinearly anisotropic coated inclusions,[29] the prediction of transport behaviors in aggregates with soft interfacial layers,[30] and the interphase description within the two-temperature model.[31]

The classical results of the homogenization theory include the variational approach,[32] leading to the Hashin–Shtrikman bounds,[33,34] and the self-consistent approach, leading to a number of effective medium schemes.[35,36] While most of the earlier theoretical activity has been devoted to particulate composites, not many investigations concern the case of the multigrained or polycrystalline microstructure with imperfect interface.[37,38] However, several nanocomposites of interest for the applications exhibit this kind of morphology,[37,38] as shown in Fig. 1. While in the particulate composite, we find two different materials with an asymmetric role, namely, dispersed particles and matrix, in multigrained systems, we have a given number of constituents with a completely symmetric role, being made of grains in close contact. Here, we propose a self-consistent homogenization method able to provide the effective transport properties of multigrained or polycrystalline materials with imperfect interfaces. In particular, we develop our theory for the case of low or high conducting interfaces, which are the typical situations observed in real systems (Fig. 1). Each grain is considered as an anisotropic material in order to
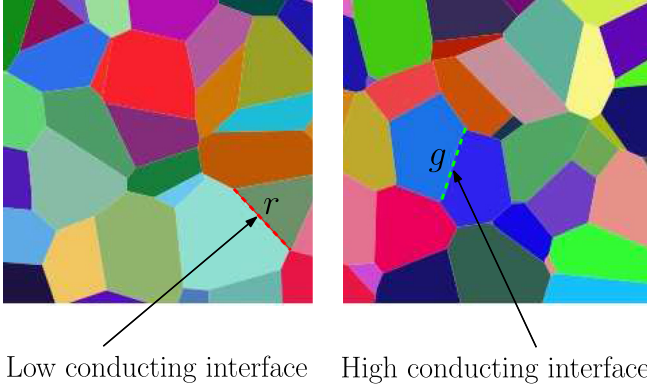
a)Electronic mail: Stefano.Giordano@iemn.univ-lille1.fr

Low conducting interface   High conducting interface

FIG. 1. Examples of a multigrained materials with imperfect interfaces. One can find low conducting interfaces described by $[\![\vec{J} \cdot \vec{n}]\!] = 0$ and $[\![\phi]\!] = -r\vec{J} \cdot \vec{n}$ or high conducting interfaces described by $[\![\phi]\!] = 0$ and $[\![\vec{J} \cdot \vec{n}]\!] = g\nabla_S^2\phi$.
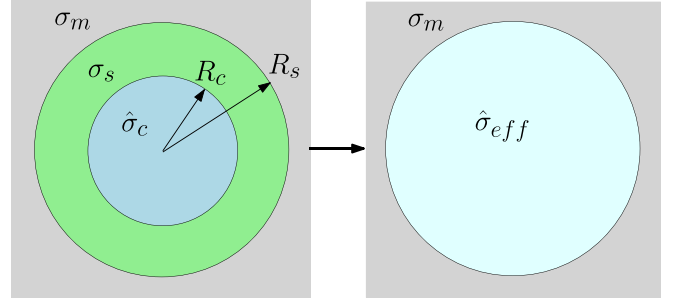

FIG. 2. Composite particle with an anisotropic core of conductivity $\hat{\sigma}_c$ (radius R_c) and an isotropic shell of conductivity σ_s (radius R_s), embedded in a matrix of conductivity σ_m. It is equivalent to a homogeneous particle of conductivity $\hat{\sigma}_{eff}$ given by Eq. (1).

mimic the real polycrystalline structure. Importantly, the results will depend on the grain size and on the statistics of contacts among the constituents. The dependence of the effective properties on the grain size makes explicit the emergence of the scale effects. On the other hand, the statistics of contacts is important to correctly describe the possible percolative behaviors. The structure of the paper is as follows. In Section II, we develop the self-consistent effective medium theory through a multiscale procedure composed of the following geometries: (i) a coated particle, (ii) a dispersion of particles with imperfect interfaces, and (iii) a multigrained system. In Section III, we present the application of the proposed theory to the analysis of the thermal conductivity of $(1 - x)$Si : xGe nanocomposites. Finally, in Section IV, we study the electric conductivity of nanocrystalline and microcrystalline $(1 - x)$Li$_2$O : xB$_2$O$_3$ composites.

II. EFFECTIVE MEDIUM THEORY

We develop here the multiscale homogenization scheme, composed of three consecutive steps, leading to the proposed effective medium theory.

A. Composite particle

To begin, we consider a composite particle in d-dimension ($d = 2$ for the cylindrical geometry and $d = 3$ for the spherical one) composed of an anisotropic core of tensor conductivity $\hat{\sigma}_c$ with radius R_c and an isotropic shell of scalar conductivity σ_s with radius R_s (see Fig. 2). In the Appendix, we prove that this composite system is equivalent to a homogeneous particle of conductivity tensor

$$\hat{\sigma}_{eff} = \sigma_s \{(d - 1)(1 - c)\sigma_s\hat{I} + [1 + c(d - 1)]\hat{\sigma}_c\} \times [(d - 1 + c)\sigma_s\hat{I} + (1 - c)\hat{\sigma}_c]^{-1}, \quad (1)$$

where c is the volume fraction of the core within the whole particle. The shell region is useful to introduce the behavior of the imperfect interface between core and matrix. To this aim, we introduce the shell width $h = R_s - R_c$, and we have $c = (R_c/R_s)^d = (1 - h/R_s)^d \simeq 1 - dh/R_s$ for small values

of h. If we consider a low conducting interface, the interface resistance is defined as[11,27]

$$r = \lim_{h \to 0, \sigma_s \to 0} \frac{h}{\sigma_s}. \quad (2)$$

Hence, in this case Eq. (1) simplifies to

$$\hat{\sigma}_{eff,LC} = \hat{\sigma}_c \left[\hat{I} + \frac{r}{R}\hat{\sigma}_c\right]^{-1}, \quad (3)$$

where $R = R_s = R_c$ under the limit of $h \to 0$. On the other hand, the interface conductance for a high conducting interface is given by[11,27]

$$g = \lim_{h \to 0, \sigma_s \to \infty} h\sigma_s. \quad (4)$$

Therefore, the effective conductivity given in Eq. (1) becomes

$$\hat{\sigma}_{eff,HC} = \hat{\sigma}_c + (d - 1)\frac{g}{R}\hat{I}, \quad (5)$$

where, again, $R = R_s = R_c$ under the limit of $h \to 0$.

This means that a single anisotropic particle with an imperfect interface can be replaced by another equivalent anisotropic particle with a perfect interface and a conductivity tensor given by Eq. (3) or Eq. (5) for LC or HC interface, respectively. We note that $\hat{\sigma}_{eff,LC}$ and $\hat{\sigma}_{eff,HC}$ depend on R. This shows the scale effects induced by the imperfect interfaces.

B. Dispersion of particles

The second step of the procedure takes into account a population of cylindrical or spherical equivalent anisotropic particles (as defined above) dispersed in a given matrix (see Fig. 3). To begin, we consider a particle of conductivity tensor $\hat{\sigma}_{eff,\xi}$ (see Eqs. (3) and (5)) embedded in a matrix of scalar conductivity σ_m (ξ stands for LC or HC depending on the type of imperfect interface considered). If we suppose to apply an external field $\vec{E}_0$ to a system composed of a single particle, we obtain the following electric field and current density inside the particle itself:

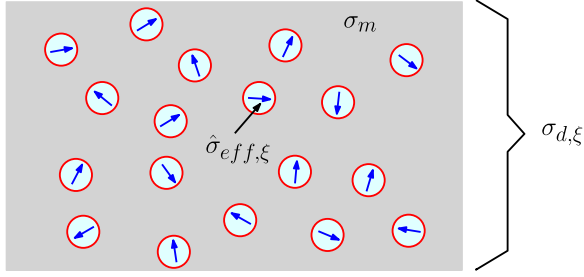$$\vec{E}_{in} = d\sigma_m[(d - 1)\sigma_m\hat{I} + \hat{\sigma}_{eff,\xi}]^{-1}\vec{E}_0, \quad (6)$$

FIG. 3. Dispersion of particles of conductivity $\hat{\sigma}_{eff,\xi}$ with volume fraction v in the matrix of conductivity σ_m. The principal conductivities $\sigma_{k,\xi}$ of $\hat{\sigma}_{eff,\xi}$ are given by $\sigma_{k,LC} = \sigma_k/(1+r\sigma_k/R)$ for low conducting interfaces and by $\sigma_{k,HC} = \sigma_k + (d-1)g/R$ for high conducting interfaces, σ_k being the eigenvalues of $\hat{\sigma}_c$.

$$\vec{J}_{in} = d\sigma_m\hat{\sigma}_{eff,\xi}[(d-1)\sigma_m\hat{I} + \hat{\sigma}_{eff,\xi}]^{-1}\vec{E}_0. \tag{7}$$

These expressions can be simply obtained through the procedure described in the Appendix, where however we impose $R_c = R_s$. Now, since we are interested in analysing a multigrained material where each anisotropic grain is randomly oriented in the space, we introduce a rotation matrix $\hat{R}$ to describe the orientation of the particle. Hence, we can write the internal fields as

$$\vec{E}_{in} = d\sigma_m\hat{R}\left[(d-1)\sigma_m\hat{I} + \hat{\sigma}_{eff,\xi}\right]^{-1}\hat{R}^T\vec{E}_0, \tag{8}$$

$$\vec{J}_{in} = d\sigma_m\hat{R}\hat{\sigma}_{eff,\xi}\left[(d-1)\sigma_m\hat{I} + \hat{\sigma}_{eff,\xi}\right]^{-1}\hat{R}^T\vec{E}_0. \tag{9}$$

The average value of the previous fields can be determined by using the expression $\langle R_{ik}R_{jk}\rangle = \delta_{ij}/d$ and by introducing the principal conductivities (eigenvalues) $\sigma_{k,\xi}$ $(k = 1, ..., d)$ of the symmetric tensor $\hat{\sigma}_{eff,\xi}$. We eventually obtain

$$\left\langle \vec{E}_{in} \right\rangle = \sigma_m\sum_{k=1}^{d}[(d-1)\sigma_m + \sigma_{k,\xi}]^{-1}\vec{E}_0, \tag{10}$$

$$\left\langle \vec{J}_{in} \right\rangle = \sigma_m\sum_{k=1}^{d}\sigma_{k,\xi}[(d-1)\sigma_m + \sigma_{k,\xi}]^{-1}\vec{E}_0, \tag{11}$$

where $\sigma_{k,\xi}$ must be substituted with $\sigma_{k,LC} = \sigma_k/(1+r\sigma_k/R)$ for low conducting interfaces and with $\sigma_{k,HC} = \sigma_k + (d-1)g/R$ for high conducting interfaces, σ_k $(k = 1, ..., d)$ being the eigenvalues of $\hat{\sigma}_c$ (see Eqs. (3) and (5)). This result represents the behavior of a randomly oriented single particle.

Now, we suppose to have a dispersion of particles with volume fraction v in the matrix of conductivity σ_m (see Fig. 3). For a dilute dispersion, we can easily determine the average value of the electric field

$$\left\langle \vec{E} \right\rangle = v\langle\vec{E}_{in}\rangle + (1-v)\vec{E}_0, \tag{12}$$

and the average value of the current density

$$\left\langle \vec{J} \right\rangle = \sigma_m\langle\vec{E}\rangle + v\langle\vec{J}_{in}\rangle - v\sigma_m\langle\vec{E}_{in}\rangle. \tag{13}$$

By combining Eqs. (12) and (13) with Eqs. (10) and (11), we can evaluate the effective conductivity $\sigma_{d,\xi}$ (defined by

$\langle\vec{J}\rangle = \sigma_{d,\xi}\langle\vec{E}\rangle$) for the dilute dispersion of randomly oriented particles

$$\sigma_{d,\xi} = \sigma_m\frac{1+(d-1)v\alpha}{1-v\alpha} \simeq \sigma_m(1+dv\alpha), \tag{14}$$

where

$$\alpha = 1 - \sum_{k=1}^{d}\frac{\sigma_m}{(d-1)\sigma_m + \sigma_{k,\xi}}, \tag{15}$$

and the approximation in Eq. (14) is valid for $v \ll 1$. This result will play a crucial role in the conclusive step of the procedure.

C. Multigrained material

We finally consider the multigrained structure, as one can see in Fig. 1. We assume to have N different materials defined by volume fractions v_i $(i = 1, ..., N, \sum_i v_i = 1)$, principal conductivities σ_k^i $(i = 1, ..., N, k = 1, ..., d)$, and average radius of grains R_i (i.e., average diameter $D_i = 2R_i$). Moreover, we suppose to know the interface resistances r_{ij} (or conductance g_{ij}) between two grains composed of materials i and j for a system with low (or high) conducting interfaces. Of course, the matrices r_{ij} and g_{ij} are symmetric. The summary of all the involved quantities can be found in Table I.

To complete the system description, we have to specify the parameter p_{ij} representing the fraction of surface of a grain of material i in contact with grains of material j. Certainly, these quantities must satisfy the normalization $\sum_j p_{ij} = 1 \forall i$. In addition, they fulfil another property which can be found as follows. We observe that the average volume of a grain of material i is $\pi^{d/2}R_i^d/\Gamma(d/2+1)$ and its average surface is $2\pi^{d/2}R_i^{d-1}/\Gamma(d/2)$, where $\Gamma(z)$ represents the Euler's Gamma function. Then, we can say that the total surface pertaining to the grains of material i is $\gamma v_i V/D_i$ with $\gamma = 4\Gamma(d/2+1)/\Gamma(d/2)$ and V is the total volume of the heterogeneous material. Therefore, the total area of material i in contact with material j is $\gamma v_i p_{ij}V/D_i$, where we used the definition of p_{ij}. The quantity $\gamma v_i p_{ij}V/D_i$ must be symmetric, and thus, we necessarily have that $v_i p_{ij}/D_i = v_j p_{ji}/D_j \forall i \neq j$. To summarize, the parameters p_{ij} satisfy the two properties

TABLE I. Definition of all the quantities involved in the self-consistent effective medium theory. See Eqs. (22)–(25).

Symbol	Definition
σ_{LC}	eff. conductivity with low conducting interfaces
σ_{HC}	eff. conductivity with high conducting interfaces
N	Number of constituents
d	Dimensionality (2 or 3)
v_i	Volume fraction of the i-th constituent
p_{ij}	Surface fraction of grain i in contact with grains j
r_{ij}	Contact resistances (LC model)
g_{ij}	Contact conductances (HC model)
D_i	Average diameter grains i
σ_k^i	Conductivity grains i in direction k
σ^i	Conductivity grains i (isotropic case)

$$\sum_{j=1}^{N} p_{ij} = 1 \; \forall i, \qquad (16)$$

$$\frac{v_i p_{ij}}{D_i} = \frac{v_j p_{ji}}{D_j} \; \forall i \neq j. \qquad (17)$$

Since Eq. (16) corresponds to N conditions and Eq. (17) corresponds to $N(N-1)/2$ conditions, we have $N^2 - N - N(N-1)/2 = N(N-1)/2$ degrees of freedom for the $N \times N$ matrix p_{ij}. In particular, when $N = 2$, we have one degree of freedom to define the 2×2 matrix p_{ij}. In the simplest case, we have no specific affinities between the materials and p_{ij} does not depend on i. Hence, in this particular case, we have that p_{ij} is proportional to v_j/D_j (i.e., to the total surface of material j) or, more precisely

$$p_{ij} = \frac{1}{\sum_{k=1}^{N} \dfrac{v_k}{D_k}} \frac{v_j}{D_j}. \qquad (18)$$

In the presence of arbitrary affinities, however, the quantities p_{ij} must fulfil Eqs. (16) and (17), in order to properly describe the statistics of the contact surfaces within the system.

We can now discuss the application of the effective medium theory to the multigrained material with imperfect interfaces. We assume to have a structure as in Fig. 1 and to know its overall effective conductivity σ_ξ (i.e., σ_{LC} or σ_{HC} depending on the type of imperfect interfaces considered). Then, we imagine to add a small grain with volume dV to the heterogeneous material (see Fig. 4). Consequently, the effective conductivity assumes the value σ'_ξ. The latter can be evaluated through Eq. (14), where $\sigma_m = \sigma_\xi$, $v = dV/V \ll 1$ and $\sigma_{k,\xi}$ describes the properties of the added grain. Therefore, we can write

$$\sigma'_\xi = \sigma_\xi \left[1 + d \frac{dV}{V} \left(1 - \sum_{k=1}^{d} \frac{\sigma_\xi}{(d-1)\sigma_\xi + \sigma_{k,\xi}} \right) \right], \qquad (19)$$

where $\sigma_{k,\xi}$ represents $\sigma_{k,LC} = \sigma_k/(1 + r\sigma_k/R)$ for low conducting interfaces and $\sigma_{k,HC} = \sigma_k + (d-1)g/R$ for high conducting interfaces, σ_k $(k = 1, ..., d)$ being the principal conductivities of the grain.

The properties of the added grain can be summed up through a vector $\vec{p}$ composed of the principal conductivities σ_k $(k = 1, ..., d)$, the radius R, and the interface parameter
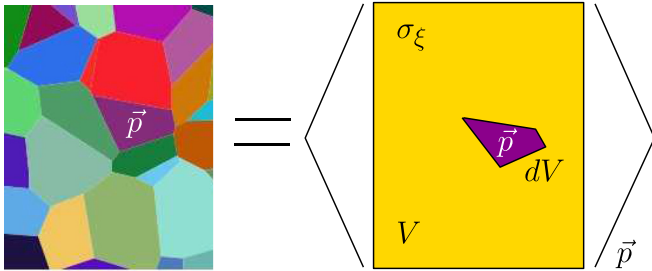

FIG. 4. Application of the effective medium theory to obtain the overall conductivity σ_ξ of the multigrained material with imperfect interfaces. The structure on the right is averaged over the properties $\vec{p} = (\sigma_k \forall k = 1, ..., d; R; r$ if $\xi = $ LC or g if $\xi = $ HC) of the added grain.

r or g, depending on the type of imperfection considered. We suppose now that the property of the added grain has been randomly attributed, self-consistently, to the same statistics of the other grains composing the heterogeneous material. It means that they have been assigned by means of the density probability

$$f(\vec{p}) = \sum_{i=1}^{N} \sum_{j=1}^{N} v_i p_{ij} \prod_{k=1}^{d} \delta(\sigma_k - \sigma_k^i) \delta\left(r - \frac{r_{ij}}{2}\right) \delta(R - R_i), \qquad (20)$$

describing low conducting interfaces. When the high conducting interfaces are considered, r and r_{ij} must be simply substituted with g and g_{ij}. To complete the procedure, we can average Eq. (19) with the density in Eq. (20). The left hand side leads to $\int_\Omega \sigma_\xi' f(\vec{p}) d\vec{p} = \sigma_\xi$, where Ω is the space where the properties $\vec{p}$ can range. It means that, if the added grain has the same statistics of the other grains, the average conductivity of the whole material remains unchanged. Therefore, the averaging of Eq. (19) yields

$$\int_\Omega \left(1 - \sum_{k=1}^{d} \frac{\sigma_\xi}{(d-1)\sigma_\xi + \sigma_{k,\xi}} \right) f(\vec{p}) d\vec{p} = 0, \qquad (21)$$

which represents the self-consistent mean field theory for our microstructure (see Fig. 4).

It is important to remark that in the first step of our procedure, we considered cylindrical ($d = 2$) or spherical ($d = 3$) particles embedded in a matrix. Then, the application of the self-consistent approach removes the concept of matrix, smearing out, at the same time, the concept of geometric shape of the particles. The average geometrical isotropy of the grains is however preserved. As a matter of fact, it is well known that the self-consistent approach is able to describe the effective behavior of microstructures represented by Voronoi tessellations.[39]

By combining Eq. (21) with Eq. (20), we straightforwardly obtain the final result for the low ($\xi = LC$) or high ($\xi = HC$) conducting interfaces

$$\frac{1}{\sigma_{LC}} = \sum_{i=1}^{N} \sum_{j=1}^{N} \sum_{k=1}^{d} \frac{v_i p_{ij}}{\dfrac{\sigma_k^i}{1 + \dfrac{r_{ij}}{D_i}\sigma_k^i} + (d-1)\sigma_{LC}}, \qquad (22)$$

$$\frac{1}{\sigma_{HC}} = \sum_{i=1}^{N} \sum_{j=1}^{N} \sum_{k=1}^{d} \frac{v_i p_{ij}}{\sigma_k^i + (d-1)\left(\dfrac{g_{ij}}{D_i} + \sigma_{HC} \right)}. \qquad (23)$$

These equations represent the main achievement of this work and allow the determination of the effective conductivity of multigrained microstructures with imperfect interfaces. We developed the whole theory by considering physically anisotropic constituents in order to present a model of large applicability, without intrinsic limitations. However, the examples discussed in the following will consider isotropic grains. In this simpler case, we have $\sigma_k^i = \sigma^i \; \forall k$ and Eqs. (22) and (23) simplify to

$$\frac{1}{d\sigma_{LC}} = \sum_{i=1}^{N}\sum_{j=1}^{N}\frac{v_i p_{ij}}{\dfrac{\sigma^i}{1+\dfrac{r_{ij}}{D_i}\sigma^i}+(d-1)\sigma_{LC}}, \qquad (24)$$

$$\frac{1}{d\sigma_{HC}} = \sum_{i=1}^{N}\sum_{j=1}^{N}\frac{v_i p_{ij}}{\sigma^i+(d-1)\left(\dfrac{g_{ij}}{D_i}+\sigma_{HC}\right)}. \qquad (25)$$

If we consider $r_{ij}=0$ and $g_{ij}=0$ in Eqs. (24) and (25), we reobtain the classical result for the effective conductivity of an isotropic random mixture without imperfect interfaces.[40,41] Similar results exist for the elastic properties of composite materials as well.[42,43]

III. THERMAL CONDUCTIVITY OF $(1-x)$ Si: xGe NANOCOMPOSITES

As an example of application of the theory for low conducting interfaces, we study the thermal conductivity of semiconductors nanocomposites, which is significantly smaller than the thermal conductivity of pure crystals. Such a strong reduction depends on the phonons scattering produced by the heterogeneity of the system, and it is here represented by an equivalent Kapitza resistance between adjacent grains. This property is exploited for improving the efficiency of semiconductors used in thermoelectric cooling, heating, and power generation.[44]

To begin, we consider a nanocomposite (multigrained material) composed of silicon (volume fraction $1-x$) and germanium (volume fraction x) grains with average size D between 5 and 100 nm. We mention that the thermal conductivity of pure crystal is $\sigma_{Si}=130$ W K^{-1} m^{-1} for silicon and $\sigma_{Ge}=58$ W K^{-1} m^{-1} for germanium. As discussed above, the marked reduction of the thermal conductivity in heterogeneous materials is taken into account through the introduction of a thermal Kapitza resistance between grains.[7] Indeed, the disordered grain boundaries generate phonon scattering preventing a good heat transfer. In this case, the effective conductivity of the composite material can be obtained through Eq. (24), applied to a system with two isotropic phases

$$\begin{aligned}\frac{1}{d\sigma_{LC}} =& \frac{(1-v_2)p_{11}}{\dfrac{\sigma_1}{1+\dfrac{r_{11}\sigma_1}{D_1}}+(d-1)\sigma_{LC}}+\frac{(1-v_2)p_{12}}{\dfrac{\sigma_1}{1+\dfrac{r_{12}\sigma_1}{D_1}}+(d-1)\sigma_{LC}} \\ &\times\frac{v_2 p_{21}}{\dfrac{\sigma_1}{1+\dfrac{r_{12}\sigma_2}{D_2}}+(d-1)\sigma_{LC}}+\frac{v_2 p_{22}}{\dfrac{\sigma_2}{1+\dfrac{r_{22}\sigma_2}{D_2}}+(d-1)\sigma_{LC}},\end{aligned}$$
$$(26)$$

where the indices 1 and 2 correspond to Si and Ge, respectively. The model allows to study both the stoichiometry and the granulometry influence on the effective conductivity. Here, we consider the case with the same average size for the Si and Ge grains, i.e., $D_1=D_2=D$. Moreover, we adopt Eq. (18) that simply leads to the expression $p_{ij}=v_j$ (we used
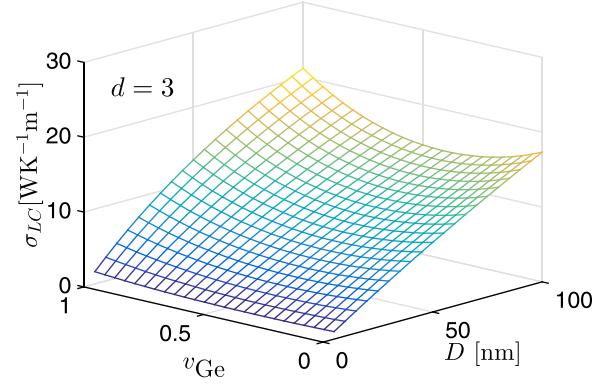

FIG. 5. Effective conductivity σ_{LC} of the multigrained Si-Ge composite versus the germanium volume fraction v_{Ge} (stoichiometry) and the average grain size D (granulometry). The surface represents the solution of Eq. (26) with $d=3$, $\sigma_{Si}=130$ W K^{-1} m^{-1}, $\sigma_{Ge}=58$ W K^{-1} m^{-1}, $r_{Si-Si}=5\times10^{-9}$ m^2 K/W, $r_{Ge-Ge}=3\times10^{-9}$ m^2 K/W, and $r_{Si-Ge}=8\times10^{-9}$ m^2 K/W.

$D_1=D_2=D$) or, more explicitly, to $p_{11}=p_{21}=v_1$ and $p_{12}=p_{22}=v_2$.

In Fig. 5, we show the general behavior of the effective thermal conductivity σ_{LC} in terms of the germanium volume fraction v_{Ge} and the average particles diameter D. We observe that the conductivity is an increasing function of D (for any value of v_{Ge}) since the fraction of grain boundaries (reducing the conductivity through the phonon scattering) is inversely proportional to the average value of D. Moreover, we note that, for a fixed value of D, the effective conductivity exhibits a minimum for $v_{Ge}=0.4-0.5$, corresponding to the largest heterogeneity of the system. This corresponds to the fact that typically the relationships $r_{Si-Ge}>r_{Si-Si}$ and $r_{Si-Ge}>r_{Ge-Ge}$ are satisfied. It means that the degradation effect of the interface is more pronounced if the adjacent grains are different.

In Fig. 6, we draw a comparison between the theoretical results based on Eq. (26), one experimental result for a
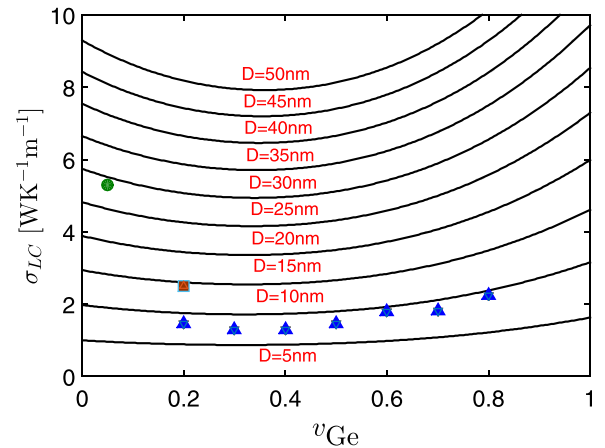

FIG. 6. Effective conductivity σ_{LC} of multigrained Si-Ge materials versus the germanium volume fraction v_{Ge} (stoichiometry) for different average grain size D (granulometry). The solid curves represent the solution of Eq. (26) with the same parameters used in Fig. 5. The red square symbol corresponds to an experimental result with $D=15$ nm and $v_{Ge}=0.2$,[45,46] the green circular symbol corresponds to another experimental result with $D=10-30$ nm and $v_{Ge}=0.05$,[47] and the blue triangles have been obtained through molecular dynamics simulations.[48]

nanocomposite with grains of size $D = 15$ nm and volume fraction $v_{Ge} = 0.2$,[45,46] and the other with $D = 10 - 30$ nm and $v_{Ge} = 0.05$,[47] and a series of molecular dynamics simulations for a system with average grain size of 10.5 nm and variable volume fraction.[48] In order to obtain the quite good agreement shown in Fig. 6, we considered the values $r_{Si-Si} = 5 \times 10^{-9}$ m^2 K/W, $r_{Ge-Ge} = 3 \times 10^{-9}$ m^2 K/W, and $r_{Si-Ge} = 8 \times 10^{-9}$ m^2 K/W for the thermal resistance between the grains. These three values represent the only quantities that we fitted in order to obtain a good agreement of the effective conductivity with the available data. Of course, the value of the Kapitza resistance depends on the nanoscopic architecture of the grain boundary and, therefore, the values adopted in our model must be considered as effective values giving the good agreement between model and existing experimental and numerical data. Interestingly enough, these values are of the same order of magnitude of other results for the thermal resistance of grain boundaries, as published in recent literature.[49–52] Therefore, this accordance confirms the applicability of our model to analyse the thermal conductivity of multigrained nanocomposites. We can also observe in Figs. 5 and 6 the thermal behavior of pure polycrystalline Si and Ge materials. Indeed, for $v_{Ge} = 0$, we have polycrystalline silicon and for $v_{Ge} = 1$ we have polycrystalline germanium, both with average grains size D. In this simple case, we easily obtain from Eq. (26) the simpler expression

$$\sigma_{LC} = \frac{\sigma_i}{1 + \dfrac{r_{ii}\sigma_i}{D}}, \tag{27}$$

which is valid for polycrystalline silicon ($i = 1$, $v_{Ge} = 0$) and polycrystalline germanium ($i = 2$, $v_{Ge} = 1$). This expression is perfectly coherent with some earlier investigations.[53–55]

To conclude, the above results about nanograined systems can be compared with the thermal conductivity of the disordered Si-Ge alloys.[56–58] We remark that the thermal conductivity is smaller in multigrained nanocomposites (with $D < 40$ nm) than in bulk alloys (where we have a plateau region for $0.2 < v_{Ge} < 0.8$).[48,56] This is coherent with the fact that in the alloy structure we have no real disordered grain boundaries between Si and Ge regions but rather a composition heterogeneity in a well defined crystal lattice. As a matter of fact, the phonons scattering effects are more pronounced in real grain boundaries than in non-homogeneous lattices. This is consistent with earlier experimental and numerical results.[45–48]

IV. ELECTRIC CONDUCTIVITY OF NANOCRYSTALLINE AND MICROCRYSTALLINE $(1-x)$ Li$_2$O : xB$_2$O$_3$ COMPOSITES

As an example of application of our theory for high conducting interfaces, we consider ionic conductors exhibiting an uncommon behavior. For instance, by reducing the grain size of the polycrystalline CaF$_2$, we can observe an increase in the overall conductivity.[59] The same phenomenon has been measured in diphase multigrain systems, where an insulator is combined with a conducting material.[60] The enhancement of

the conductivity has a practical interest since these ionic conductors are suitable electrolytes in solid-state batteries. Recent studies concern the measurement of conductivity in nanocrystalline and microcrystalline $(1 - x)$Li$_2$O: xB$_2$O$_3$ composites, where Li$_2$O is an ionic conductor and B$_2$O$_3$ is an insulator.[61,62] The improved conductivity leads to a pronounced maximum in the effective conductivity versus the volume fraction of the insulator phase. This maximum is followed by a percolation phenomenon characterized by a percolation threshold and a zero conductivity. This behavior can be explained by assuming that at the Li$_2$O $-$ B$_2$O$_3$ interfaces the conductivity is strongly enhanced and it can be therefore described by the high conducting interface model. Indeed, the conductivity intensification is more pronounced for smaller grain size, being in this case larger the total contact area between Li$_2$O and B$_2$O$_3$. Experiments showed that, at a temperature of 433 K, we have $\sigma_{LiO_2} \cong 5 \times 10^{-8}$ S/cm and $\sigma_{B_2O_3}$ quite negligible. Therefore, we define $\sigma_1 = \sigma_{B_2O_3} = 0$ S/cm and $\sigma_2 = \sigma_{LiO_2} = 5 \times 10^{-8}$ S/cm. We also define the volume fractions $v_1 = v_{B_2O_3} = v$, $v_2 = v_{LiO_2} = 1 - v$ and the dimensionless effective conductivity $y = \sigma_{HC}/\sigma_{LiO_2}$ (see Eqs. (23) and (25) for the definition of σ_{HC}). We suppose to have the same average size for conducting and insulating grains, i.e., $D_1 = D_2 = D$, coherently with experimental data.[61,62] The Li$_2$O $-$ B$_2$O$_3$ interphase is characterized by a conductivity $\sigma_{high}/\sigma_{LiO_2} = 200$ and by a thickness $\lambda = 1$ nm, independently of the grain size.[61,62] Hence, we can use Eq. (4) in order to define the value of the interface conductance g. We easily find the general expression $g = \lambda\sigma_{high}$, where λ is the interface thickness and σ_{high} represents its conductivity. This mixture shows specific size dependent affinities between the two components, which are not taken into account by Eq. (18). So, in order to apply Eq. (25) to this heterogeneous system, we search for the most general form of the matrix p_{ij} for a diphase system with $D_1 = D_2 = D$. As above discussed, this 2×2 matrix has only one degree of freedom since it must satisfy Eqs. (16) and (17). So, if we set $p_{11} = \alpha v$ (p_{11} must be proportional to the insulator volume fraction), we easily find that

$$\begin{pmatrix} p_{11} & p_{12} \\ p_{21} & p_{22} \end{pmatrix} = \begin{pmatrix} \alpha v & 1 - \alpha v \\ \dfrac{v(1-\alpha v)}{1-v} & \dfrac{1-2v+\alpha v^2}{1-v} \end{pmatrix}. \tag{28}$$

Of course, when $\alpha = 1$ we obtain the simpler scheme characterized by Eq. (18). Anyway, the application of Eq. (25) leads to

$$\frac{1}{dy} = \frac{\alpha v^2}{(d-1)y} + \frac{1 - 2v + \alpha v^2}{1 + (d-1)y} + \frac{v(1-\alpha v)}{(d-1)(y+\beta)} + \frac{v(1-\alpha v)}{1 + (d-1)(y+\beta)}, \tag{29}$$

where $\beta = g/(\sigma_{LiO_2}D) = \lambda\sigma_{high}/(\sigma_{LiO_2}D)$ depends on both the granulometry and the interface conductance.

The behavior described by Eq. (29) can be found in Figs. 7 and 8. In Fig. 7, we consider the case with $\alpha = 1$ and a variable coefficient β, and we plot the normalized effective conductivity y for two-and three-dimensional structures. We observe that the percolation behavior depends only on the
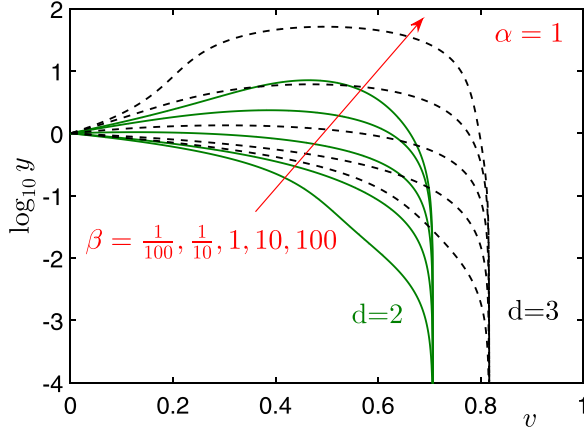
FIG. 7. Solutions of Eq. (29) with fixed α and variable β for both $d = 2$ and $d = 3$. The percolation threshold depends only on the dimensionality of the system.

FIG. 9. Comparison between solutions of Eq. (29) (solid lines) and experimental data (symbols) for microscopic and nanoscopic grains.[61,62] While for $D = 10~\mu m$ we have a decreasing behavior of the effective conductivity versus the insulator volume fraction, for $D = 20~nm$ we have a maximum of the conductivity and a larger percolation threshold.

dimensionality of the system. Indeed, we can easily deduce from Eq. (29) that the percolation threshold is given by

$$v^* = \sqrt{\frac{d-1}{\alpha d}}, \qquad (30)$$

depending only on α and d. It is interesting to note that the coefficient β controls the emergence of a maximum point in the conductivity curves. Being β inversely proportional to the average grain size D, we underline that the maximum is more pronounced for nanoscopic grains. In previous literature, this behavior has been clearly observed by using Monte-Carlo simulations for percolating systems with high conducting interfaces.[63]

Conversely, in Fig. 8, we show the results obtained by setting $\beta = 10$ and by varying α in the range from 0.8 to 1.2. In this case, we observe a shift of the percolation threshold, as predicted by Eq. (30). From the physical point of view, this point can be explained by observing that p_{ij} (or α) defines the statistics of the contacts between different grains and, therefore, controls the conducting paths within the composite system. Consequently, the value of α is directly correlated with the percolation properties of the system.
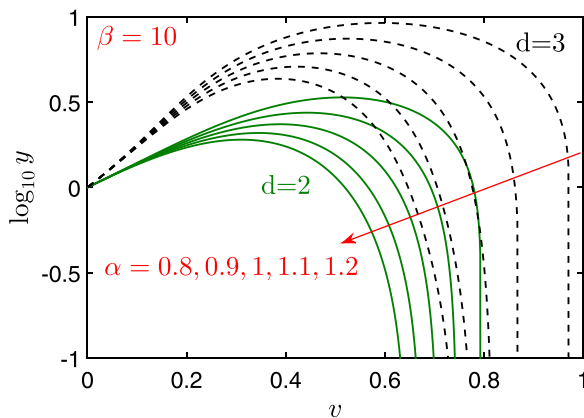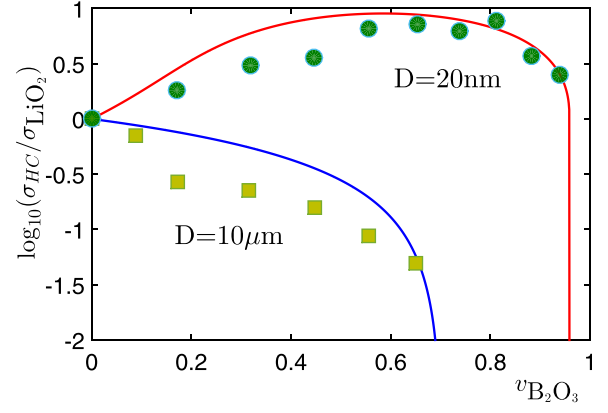
Finally, in Fig. 9, the theoretical results have been accurately confirmed against available experimental data concerning the $(1-x)\text{Li}_2\text{O} : x\text{B}_2\text{O}_3$ system with microscopic and nanoscopic grains.[61,62] The microscopic grains have an average size $D = 10~\mu m$, and therefore, we have $\beta = 2 \times 10^{-2}$. The quite good agreement with the experimental data has been obtained with $\alpha = 1.36$. For the nanoscopic grains, we have $D = 20~nm$ and $\beta = 10$, and we used the value $\alpha = 0.81$. We note that the model is able to predict the broad maximum of the conductivity for $v_{\text{B}_2\text{O}_3} \simeq 0.6$ in the case of nanoscopic grains and the monotone decreasing behavior of the conductivity for the case of microscopic grains. Moreover, the introduction of the coefficients p_{ij} allowed the perfect interpretation of the percolation threshold positions. This point has been realized through the associated coefficient α, which is the sole free parameter (not fixed by known physical quantities) in this comparison of theoretical and experimental results.

V. CONCLUSION

In this paper, we presented a generalization of the effective medium theory explicitly developed for taking into account the effects of imperfect interfaces in multigrained (polycrystalline) composite materials. More specifically, we considered both the low conducting and the high conducting imperfect interfaces. To approach the problem, we proposed a multiscale procedure composed of the following steps: (i) at the beginning, we considered a coated particle and we analysed the limiting cases of low and high conducting interfaces; (ii) then, we determined the effective conductivity of a dispersion of particles with imperfect interfaces; (iii) finally, we implemented a self-consistent effective medium theory to move from dispersions to multigrained systems. The theoretical results have been compared with numerical and experimental data concerning the thermal conductivity of $(1-x)\text{Si} : x\text{Ge}$ mixtures and the electrical conductivity of $(1-x)\text{Li}_2\text{O} : x\text{B}_2\text{O}_3$ composites. In both cases, we found a good agreement between theory and earlier results.

FIG. 8. Solutions of Eq. (29) with fixed β and variable α for both $d = 2$ and $d = 3$. The percolation threshold depends on the dimensionality of the system and on the value of α, as predicted by Eq. (30).

APPENDIX: CORE-SHELL STRUCTURE HOMOGENIZATION

We consider a core-shell structure in d-dimension composed of an anisotropic core of tensor conductivity $\hat{\sigma}_c$ with radius R_c and an isotropic shell of scalar conductivity σ_s with radius R_s (see Fig. 2). We embed this composite particle in a matrix with conductivity σ_m, where an external uniform electric field $\vec{E}_0$ is applied. We use the terminology typical of the electrical conductivity context, but we know that the results can be applied to all other transport processes as well. We consider the following mathematical form of the electrical potential in the three regions (core, shell, and matrix)

$$\phi_m = -\vec{E}_0 \cdot \vec{x} + \frac{\vec{Q} \cdot \vec{x}}{r^d}, \tag{A1}$$

$$\phi_s = \vec{S} \cdot \vec{x} + \frac{\vec{T} \cdot \vec{x}}{r^d}, \tag{A2}$$

$$\phi_c = \vec{C} \cdot \vec{x}, \tag{A3}$$

where $\vec{x} = (x_1, x_2, x_3)$ is the position vector, $r = ||\vec{x}||$, and $d = 2$ or 3 depending on the cylindrical or spherical geometry considered. As well known, the dipolar term $\vec{a} \cdot \vec{x}/r^d$ satisfies the Laplace equation $\forall \vec{a}$, i.e., $\nabla_d^2(\vec{a} \cdot \vec{x}/r^d) = 0$, where $\nabla_d^2 = \sum_{i=1}^{d} \partial_{x_i} \partial_{x_i}$. The unknown vectors $\vec{Q}$, $\vec{S}$, $\vec{T}$, and $\vec{C}$ must be determined by considering the continuity of the electrical potential and of the normal component of the displacement vector over the two surfaces with radii R_c and R_s. After long but straightforward calculations, the four conditions can be written as follows:

$$\vec{C} = \vec{S} + \frac{\vec{T}}{R_c^d}, \tag{A4}$$

$$-\vec{E}_0 + \frac{\vec{Q}}{R_s^d} = \vec{S} + \frac{\vec{T}}{R_s^d}, \tag{A5}$$

$$\hat{\sigma}_c \vec{C} = \sigma_s \vec{S} - \sigma_s (d-1) \frac{\vec{T}}{R_c^d}, \tag{A6}$$

$$\sigma_s \vec{S} - \sigma_s (d-1) \frac{\vec{T}}{R_s^d} = -\sigma_m \vec{E}_0 - \sigma_m (d-1) \frac{\vec{Q}}{R_s^d}. \tag{A7}$$

In order to homogenize the composite particle, we need to analyse the external field described by the vector coefficient $\vec{Q}$. Its value can be found by solving the system composed of Eqs. (A4)–(A7), eventually obtaining

$$\vec{Q} = \hat{N} \hat{D}^{-1} \vec{E}_0, \tag{A8}$$

where

$$\hat{N} = R_s^d \left\{ \left(\frac{R_s}{R_c}\right)^d (\sigma_s - \sigma_m) \left[\sigma_s(d-1)\hat{I} + \hat{\sigma}_c\right] \right.$$

$$\left. + [\sigma_s(d-1) + \sigma_m](\hat{\sigma}_c - \sigma_s \hat{I}) \right\}, \tag{A9}$$

$$\hat{D} = \left(\frac{R_s}{R_c}\right)^d [\sigma_s + (d-1)\sigma_m] [\sigma_s(d-1)\hat{I} + \hat{\sigma}_c]$$

$$+ (d-1)(\sigma_s - \sigma_m)(\hat{\sigma}_c - \sigma_s \hat{I}). \tag{A10}$$

If we consider the particular case of a homogeneous particle of tensor conductivity $\hat{\sigma}_{eff}$, we can determine the corresponding value of $\vec{Q}$ by considering $R_c = R_s$ and $\hat{\sigma}_c = \hat{\sigma}_{eff}$ in Eq. (A8). The result is

$$\vec{Q}\left(\begin{array}{c} R_c = R_s \\ \hat{\sigma}_c = \hat{\sigma}_{eff} \end{array}\right) = R_s^d (\hat{\sigma}_{eff} - \sigma_m \hat{I})$$

$$\times [\sigma_m(d-1)\hat{I} + \hat{\sigma}_{eff}]^{-1} \vec{E}_0. \tag{A11}$$

The effective conductivity tensor $\hat{\sigma}_{eff}$ of the composite particle is defined as the conductivity tensor of an homogeneous particle that generates the same external field of the composite one. Hence, we can find $\hat{\sigma}_{eff}$ by equating Eqs. (A8) and (A11), and the final result is

$$\hat{\sigma}_{eff} = \sigma_m(\hat{D} + (d-1)\hat{N})(\hat{D} - \hat{N})^{-1}$$

$$= \sigma_s \{ (d-1)(1-c)\sigma_s \hat{I} + [1 + c(d-1)]\hat{\sigma}_c \}$$

$$\times [(d-1+c)\sigma_s \hat{I} + (1-c)\hat{\sigma}_c]^{-1}. \tag{A12}$$

Of course, we can observe that $\hat{\sigma}_{eff}$ does not depend on σ_m, as expected.

[1]S. Torquato, *Random Heterogeneous Materials* (Springer-Verlag, New York, 2002).
[2]G. W. Milton, *The Theory of Composites* (Cambridge University Press, Cambridge, 2002).
[3]S. Kanaun and V. Levin, *Self-Consistent Methods for Composites*, Static Problems Vol. 1 (Springer, Dordrecht, 2008).
[4]S. Kanaun and V. Levin, *Self-Consistent Methods for Composites*, Wave Propagation in Heterogeneous Materials Vol. 2 (Springer, Dordrecht, 2008).
[5]J. A. Stratton, *Electromagnetic Theory* (McGraw Hill, New York, 1941).
[6]L. D. Landau and E. M. Lifshitz, *Electrodynamics of Continuous Media* (Pergamon Press, London, 1984).
[7]P. L. Kapitza, *Collected Papers of P.L. Kapitza* (Pergamon Press, Oxford, 1964–1967), Vol. 3.
[8]Y. Benveniste and T. Miloh, Int. J. Eng. Sci. **24**, 1537 (1986).
[9]Y. Benveniste, J. Appl. Phys. **61**, 2840 (1987).
[10]D. P. H. Hasselman and L. F. Johnson, J. Compos. Mater. **21**, 508 (1987).
[11]S. Torquato and M. D. Rintoul, Phys. Rev. Lett. **75**, 4067 (1995).
[12]R. Lipton and B. Vernescu, Proc. R. Soc. London, Ser. A **452**, 329 (1996).
[13]R. Lipton and B. Vernescu, J. Appl. Phys. **79**, 8964 (1996).
[14]H. Cheng and S. Torquato, Proc. R. Soc. London, Ser. A **453**, 145 (1997).
[15]C.-W. Nan, R. Birringer, D. R. Clarke, and H. Gleiter, J. Appl. Phys. **81**, 6692 (1997).
[16]Z. Hashin, J. Appl. Phys. **89**, 2261 (2001).
[17]H. L. Duan and B. L. Karihaloo, Phys. Rev. B **75**, 064206 (2007).
[18]H. Le Quang, Q.-C. He, and G. Bonnet, Philos. Mag. **91**, 3358 (2011).
[19]R. Lipton, SIAM J. Appl. Math. **57**, 347 (1997).
[20]R. Lipton, J. Mech. Phys. Solids **45**, 361 (1997).
[21]T. Miloh and Y. Benveniste, Proc. R. Soc. London, Ser. A **455**, 2687 (1999).
[22]J. Yvonnet, Q.-C. He, and C. Toulemonde, Compos. Sci. Technol. **68**, 2818 (2008).
[23]H. Le Quang, G. Bonnet, and Q.-C. He, Phys. Rev. B **81**, 064203 (2010).
[24]Y. Benveniste, J. Mech. Phys. Solids **54**, 708 (2006).
[25]Y. Benveniste, Proc. R. Soc. London, Ser. A **462**, 1593 (2006).
[26]S. T. Gu and Q. C. He, J. Mech. Phys. Solids **59**, 1413 (2011).
[27]F. Pavanello, F. Manca, P. L. Palla, and S. Giordano, J. Appl. Phys. **112**, 084306 (2012).
[28]F. Pavanello and S. Giordano, J. Appl. Phys. **113**, 154310 (2013).

[29]Y. Benveniste, Int. J. Eng. Sci. **72**, 140 (2013)

[30]W. Xu, H. Chen, W. Chen, and L. Jiang, Soft Matter **10**, 627 (2014).

[31]S. Giordano and F. Manca, Int. J. Heat Mass Transfer **78**, 189 (2014).

[32]Z. Hashin and S. Shtrikman, Phys. Rev. **130**, 129 (1963).

[33]Z. Hashin and S. Shtrikman, J. Appl. Phys. **33**, 3125 (1962).

[34]Z. Hashin and S. Shtrikman, J. Mech. Phys. Solids **10**, 335 (1962).

[35]D. J. Bergman and D. Stroud, Solid State Phys. **46**, 147 (1992).

[36]D. Stroud, Superlattices Microstruct. **23**, 567 (1998).

[37]M. Sahimi, *Heterogeneous Materials I, Linear Transport and Optical Properties* (Springer-Verlag, New York, 2003).

[38]M. Sahimi, *Heterogeneous Materials II, Nonlinear and Breakdown Properties and Atomistic Modeling* (Springer-Verlag, New York, 2003).

[39]L. Colombo and S. Giordano, Rep. Prog. Phys. **74**, 116501 (2011).

[40]B. Bianco and S. Giordano, Int. J. Circuit Theory Appl. **31**, 199 (2003).

[41]S. Giordano, Int. J. Circuit Theory Appl. **33**, 519 (2005)

[42]E. Kröner, J. Phys. F: Met. Phys. **8**, 2261 (1978).

[43]S. Giordano, ASME J. Eng. Mater. Technol. **129**, 453 (2007).

[44]M. S. Dresselhaus, G. Chen, M. Y. Tang, R. Yang, H. Lee, D. Wang, Z. Ren, J.-P. Fleurial, and P. Gogna, Adv. Mater. **19**, 1043 (2007).

[45]X. W. Wang, H. Lee, Y. C. Lan, G. H. Zhu, G. Joshi, D. Z. Wang, J. Yang, A. J. Muto, M. Y. Tang, J. Klatsky, S. Song, M. S. Dresselhaus, G. Chen, and Z. F. Ren, Appl. Phys. Lett. **93**, 193121 (2008).

[46]G. Joshi, H. Lee, Y. Lan, X. Wang, G. Zhu, D. Wang, R. W. Gould, D. C. Cuff, M. Y. Tang, M. S. Dresselhaus, G. Chen, and Z. Ren, Nano Lett. **8**, 4670 (2008).

[47]G. H. Zhu, H. Lee, Y. C. Lan, X. W. Wang, G. Joshi, D. Z. Wang, J. Yang, D. Vashaee, H. Guilbert, A. Pillitteri, M. S. Dresselhaus, G. Chen, and Z. F. Ren, Phys. Rev. Lett. **102**, 196803 (2009).

[48]C. Melis and L. Colombo, Phys. Rev. Lett. **112**, 065901 (2014).

[49]S. Aubry, C. J. Kimmer, A. Skye, and P. K. Schelling, Phys. Rev. B **78**, 064112 (2008).

[50]E. S. Landry and A. J. H. McGaughey, Phys. Rev. B **80**, 165304 (2009).

[51]K. R. Hahn, M. Puligheddu, and L. Colombo, Phys. Rev. B **91**, 195313 (2015).

[52]R. Dettori, C. Melis, X. Cartoixá, R. Rurali, and L. Colombo, Adv. Phys. X **1**, 246 (2016).

[53]C.-W. Nan and R. Birringer, Phys. Rev. B **57**, 8264 (1998).

[54]H.-S. Yang, G.-R. Bai, L. J. Thompson, and J. A. Eastman, Acta Mater. **50**, 2309 (2002).

[55]J.-P. Crocombette and L. Gelebart, J. Appl. Phys. **106**, 083520 (2009).

[56]J. Garg, N. Bonini, B. Kozinsky, and N. Marzari, Phys. Rev. Lett. **106**, 045901 (2011).

[57]H. Stohr and W. Klemm, Z. Anorg. Allg. Chem. **241**, 305 (1939).

[58]B. Abeles *et al.*, Phys. Rev. **125**, 44 (1962).

[59]W. Puin and P. Heitjans, Nanostruct. Mater. **6**, 885 (1995).

[60]C. C. Liang, J. Electrochem. Soc. **120**, 1289 (1973).

[61]S. Indris, P. Heitjans, H. E. Roman, and A. Bunde, Phys. Rev. Lett. **84**, 2889 (2000).

[62]M. Ulrich, A. Bunde, S. Indris, and P. Heitjans, Phys. Chem. Chem. Phys. **6**, 3680 (2004).

[63]A. Bunde, W. Dieterich, and E. Roman, Phys. Rev. Lett. **55**, 5 (1985).